Electronic Charge Transport in Extended Nematic Liquid Crystals

Kai L. Woon,[†] Matthew P. Aldred,[‡] Panos Vlachos,[‡] Georg H. Mehl,[‡] Tom Stirner,[‡] Stephen M. Kelly,*[,‡] and Mary O'Neill*[,†]

Department of Physics and Department of Chemistry, University of Hull, Cottingham Road, Hull HU6 7RX, United Kingdom

Received January 19, 2006

We report a systematic study of charge transport in a range of low-molar-mass and extended (having at least six aromatic rings) nematic liquid crystals, some of which are reactive mesogens, with a high degree of shape anisotropy, i.e., the length-to-width (aspect) ratio is exceptionally high. We demonstrate that the hole mobility is independent of the macroscopic, but not microscopic, ordering of the nematic and isotropic phases of these nematic liquid crystals with a long, rigid, and extended aromatic molecular core, because no discontinuity is observed at the transition between these phases. A room-temperature mobility of up to 1.0×10^{-3} cm^2 V^{-1} s^{-1} is obtained in the nematic phase, which is attributed to the short intermolecular distances between the highly polarizable but rigid long aromatic cores. We show that the intermolecular separation can be easily fine-tuned by changing the lateral and terminal aliphatic groups of these nematic liquid crystals. Hence, the charge mobility can be varied by up to 2 orders of magnitude without altering the core structure of the molecules, and this chemical fine control could be used to limit hole transport and so provide better charge balance in organic light-emitting diodes. X-ray diffraction is used to obtain the intermolecular separation and shows local lamellar order in the nematic phase.

I. Introduction

Advances in the area of organic electronics, such as organic light-emitting diodes (OLEDs), require an understanding of the structural influence of the organic material on the nature and magnitude of the charge transport. Such an understanding would provide a design guidance for molecular synthesis in order to assist the further commercialization and market penetration of these technologies. Liquid crystals (LCs) in general, e.g., smectic, discotic columnar, and nematic liquid crystals, have the potential to become an important class of electronic charge-transporting materials soon. The charge-transport properties of discotic[1−3] and smectic LCs[4−7] have been studied extensively with obtained carrier mobility values of up to 0.4 and 0.1 cm^2 V^{-1} s^{-1} , measured by a pulse−radiolysis time-resolved microwave conductivity technique and time of flight, respectively.[1,4] A recent breakthrough in the applicability of these materials is the observation of smectic and discotic phases at room temperature.[4,8] However, liquid crystals are fluids and so may not be robust or morphologically stable enough for long-term use in thin-film devices in the liquid crystalline state. A very promising solution to this problem is the in situ photopolymerization and cross-linking of semiconducting liquid crystals with photoreactive end groups (reactive mesogens) to form an insoluble polymer network as a uniform thin film. Thin films of highly crosslinked discotic and nematic polymer networks have been used as charge transport and light-emitting layers, respectively, in OLEDs.[9,10] More recently, smectic polymer networks have formed the transport layer of organic thin-film transistors.[7] However, although the hole mobility of nematic materials increases following photopolymerization,[11] the opposite is true for smectics and discotics.[7,12] This is not surprising, as the positional order in terms of a layered or columnar structure of the latter types of thermotropic liquid crystals is disrupted when the end chains are polymerized to form a network of interlinked polymer backbones with their own space-filling and conformational requirements. Recently, nematic polymer networks have been shown to generate

* To whom correspondence should be addressed. E-mail: s.m.kelly@hull.ac.uk (S.M.K.); m.oneill@hull.ac.uk (M.O.).
[†] Department of Physics, University of Hull.
[‡] Deparment of Chemistry, University of Hull.

(1) Debije, M. G.; Piris, J.; de Haas, M. P.; Warman, J. M.; Tomovic, Z.; Simpson, C. D.; Watson, M. D.; Müllen, K. *J. Am. Chem. Soc*. **2004**, *126*, 4641.
(2) Adam, D.; Schuhmacher, P.; Simmerer, J.; Haussling, L.; Siemensmeyer, K.; Etzbach, K. H.; Ringsdorf, H.; Haarer, D. *Nature* **1994**, *371*, 141.
(3) (a) Bushby, R. J.; Lozman, O. R. *Curr. Opin. Solid State Mater.* **2003**, *6*, 569. (b) O'Neill, M.; Kelly, S. M. *Adv. Mater.* **2003**, *15*, 1135.
(4) Funahashi, M.; Hanna, J. I. *Adv. Mater.* **2005**, *17*, 594.
(5) Funahashi, M.; Hanna, J. I. *Appl. Phys. Lett.* **2000**, *76*, 2574.
(6) Vlachos, P.; Kelly, S. M.; Mansoor, B.; O'Neill, M. *Chem. Commun.* **2002**, 874.
(7) McCulloch, I.; Zhang, W.; Heeney, M.; Bailey, C.; Giles, M.; Graham, D.; Shkunov, M.; Sparrowe, D.; Tierney, S. *J. Mater. Chem.* **2003**, *13*, 2436.
(8) Liu, C.-Y.; Fechtenkotter, A.; Watson, M. D.; Müllen, K.; Bard, A. J. *Chem. Mater.* **2003**, *15*, 124.
(9) Bacher, A.; Erdelen, C. H.; Paulus, W.; Ringsdorf, H.; Schmidt, H.-W.; Schuhmacher, P. *Macromolecules* **1999**, *32*, 4551.
(10) Contoret, A. E. A.; Farrar, S. R.; Jackson, P. O.; Khan, S. M.; May, L.; O'Neill, M.; Nicholls, J. E.; Kelly, S. M.; Richards, G. J. *Adv. Mater.* **2000**, *12*, 971.
(11) Farrar, S. R.; Contoret, A. E. A.; O'Neill, M.; Nicholls, J. E.; Richards, G. J.; Kelly, S. M. *Phys. Rev. B* **2002**, *66*, 125107.
(12) Bleyl, I.; Erdelen, C.; Etzbach, K. H.; Paulus, W.; Schmidt, H. W.; Siemensmeyer, K.; Haarer, D. *Mol. Cryst. Liq. Cryst. A* **1997**, *299*, 149.

10.1021/cm0601335 CCC: $33.50
Published on Web 03/29/2006

efficient electroluminescence, e.g., with an efficacy of 6.8 cd A^{-1}, and a pixellated red, green, and blue OLED has been fabricated using photolithography in conjunction with nematic polymer networks.[13,14] Therefore, charge-transporting nematic liquid crystals are certainly worthy of further study and development. However, despite these promising device properties and the potential of much higher mobility values for nematic liquid crystals of this type, there are few studies on the electronic charge-transport properties of low-molar-mass nematic liquid crystals in general and this type of nematic liquid crystal in particular. It should be noted that we distinguish here between low-molar-mass nematics and much longer oligomeric nematic glasses, which also show considerable promise for OLEDs and organic transistors, for example.[15,16]

Initial reports suggested that ionic, rather than electronic, conduction occurs in nematic LCs designed with a short, polar aromatic core, inducing a low viscosity for use in LCDs.[17,18] The more recently developed light-emitting nematic LCs with a very long, apolar aromatic core with a high degree of conjugation were designed for use in OLEDs and give rise to bright electroluminescence, showing that charge transport must indeed be electronic rather than ionic.[10] So far, extended nematic LCs with a large aspect ratio mostly exhibit hole transport with only moderate mobility.[11]

The transition temperatures of LCs depend on the length and shape of aliphatic end groups in a terminal position and the nature, number, and position of lateral substituents. This correlation is primarily attributed to steric effects, i.e., these molecular units influence the intermolecular separation in the nematic phase. However, the electronic charge transport, which proceeds by a series of intermolecular hops, should also depend on the intermolecular separation in a related fashion. Therefore, the study of a small number of carefully designed, highly polarizable, nonpolar nematic LCs with a high aspect ratio and different lateral and terminal substituents should generate an insight into charge transport through nematic LCs. A better understanding of this relationship would facilitate the synthesis of nematic liquid crystals with a high absolute value of the charge mobility of holes and perhaps electrons, which would then improve the performance of a range of practical electro-optic devices using organic semiconductors. So, we now report a systematic study of the dependence on the intermolecular separation of charge transport in extended nematic liquid crystals with a high degree of shape anisotropy that can be prepared as monomers (reactive mesogens) for the fabrication of nematic polymer networks by photolithography techniques for use in more efficient OLEDs with balanced charge density, for example.

Table 1. Chemical Structures and Transition Temperatures of Compounds 1−7

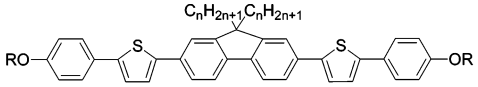

	OR [= RO]	n	T_g		Cr		N		I
1	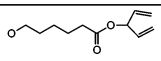	3	•	39	•	92	•	108	•
2	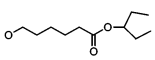	3	•	32	•	109	(•	100)	•
3	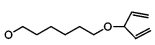	3	•	19	•	92	•	116	•
4	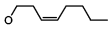	3	•	32	•	153	(•	146)	•
5	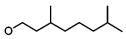	3	•	20	•	110	•	124	•
6		8	•	-12	•	69	•	99	•
7	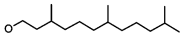	8	•	-17	•	44	(•	16)	•

Parentheses denote monotropic mesophase

Table 2. Chemical Structures and Transition Temperatures of Compounds 8 and 9

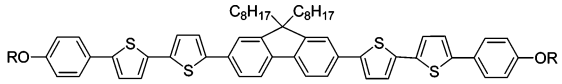

	OR [= RO]	T_g		Cr		N		I
8	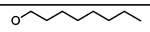	•	45	•	118	•	210	•
9	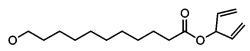	•	0	•	52	•	143	•

II. Experimental Section

Materials Synthesis. The generic methods of synthesis of compounds **1**−**7**, collated in Table 1, have been reported elsewhere.[19,20] The synthesis of compounds **8** and **9**, shown in Table 2, is shown in Scheme 1. The structures of intermediates and final products were confirmed by proton (^{1}H) nuclear magnetic resonance (NMR) spectroscopy, infrared (IR) spectroscopy, and mass spectrometry (MS). All commercially available starting materials, reagents, and solvents were used as supplied, unless otherwise stated, and were obtained from Aldrich, Strem Chem Inc., Acros, or Lancaster Synthesis. Tetrahydrofuran was predried with sodium wire and then distilled over sodium wire under nitrogen with a benzophenone indicator when required and was not stored. All reactions were carried out using a dry nitrogen atmosphere unless water was present as solvent or reagent, and the temperatures were measured externally. For compounds with RMM < 800 g mol^{-1}, mass spectra were recorded using a Schimadzu QP5050A gas chromatography/mass spectrometer with electron impact (EI) at a source temperature of 200 °C. For compounds with RMM > 800 g mol^{-1}, mass spectra were analyzed using a Bruker reflex IV matrix-assisted laser desorption/ionization (MALDI) time-of-flight (TOF) MS. A 384-well microliter plate format was used with a

(13) Aldred, M. P.; Contoret, A. E. A.; Devine, P. E.; Farrar, S. R.; Hudson, R.; Kelly, S. M.; Koch, G. C.; O'Neill, M.; Tsoi, W. C.; Woon, K. L.; Vlachos, P. *Mater. Res. Soc. Symp. Proc.* **2005**, *871E*, I10.7.
(14) Aldred, M. P.; Contoret, A. E. A.; Farrar, S. R.; Kelly, S. M.; Mathieson, D.; O'Neill, M.; Tsoi, W. C.; Vlachos, P. *Adv. Mater.* **2005**, *17*, 1368.
(15) Geng, Y.; Chen, A. C. A.; Ou, J. J.; Chen, S. H.; Klubek, K.; Vaeth, K. M.; Tang, C. W. *Chem. Mater.* **2003**, *15*, 4352.
(16) Yasuda, T.; Fujita, K.; Tsutsui, T.; Geng, Y. H.; Culligan, S. W.; Chen, S. H. *Chem. Mater.* **2005**, *17*, 204.
(17) Sugimura, A.; Matsui, N.; Takahashi, Y.; Sonomura, H.; Okuda, M. *Phys. Rev. B* **1991**, *43*, 8272.
(18) Murakami, S.; Naito, H.; Okuda, M.; Sugimura, A. *J. Appl. Phys.* **1995**, *78*, 4533.
(19) Contoret, A. E. A.; Farrar, S. R.; O'Neill, M.; Nicholls, J. E.; Richards, G. J.; Kelly, S. M.; Hall, A. W. *Chem. Mater.* **2002**, *14*, 1477.
(20) Aldred, M. P.; Eastwood, A. J.; Kelly, S. M.; Vlachos, P.; Contoret, A. E. A.; Farrar, S. R.; Mansoor, B.; O'Neill, M.; Tsoi, W. C. *Chem. Mater.* **2004**, *16*, 4928.

Scheme 1[a]

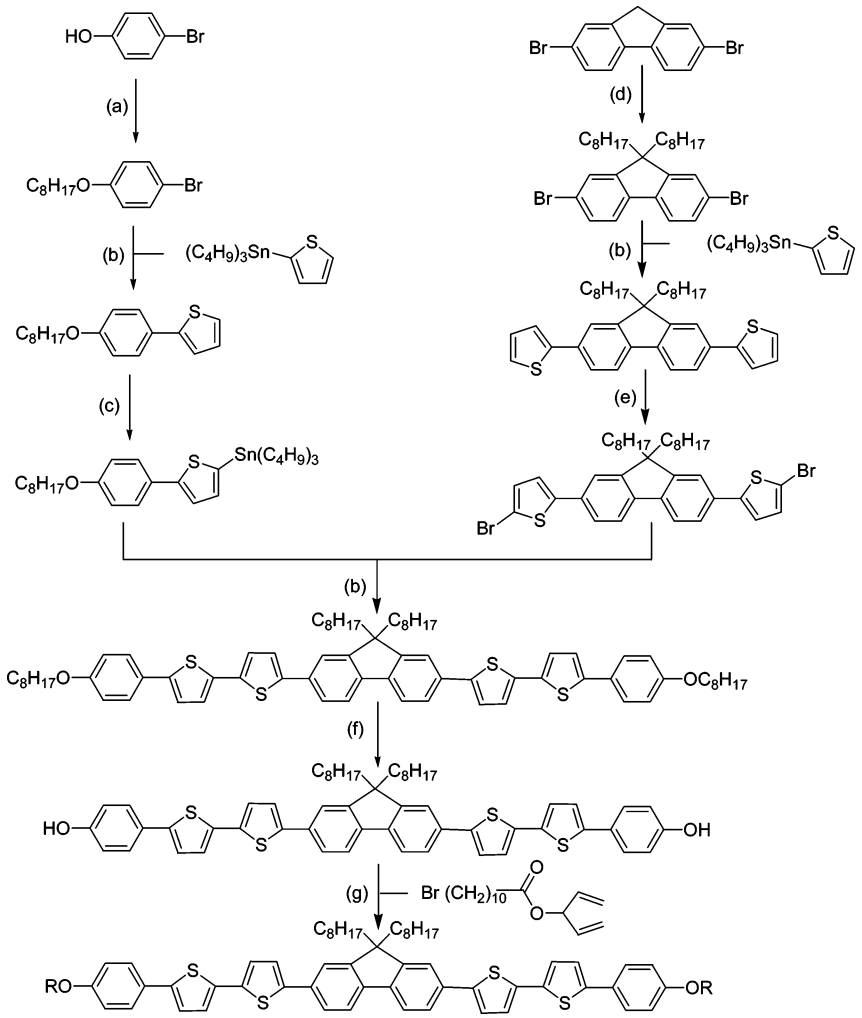

[a] Reagents: (a) K_2CO_3, $CH_3COC_2H_5$, $C_8H_{17}Br$ (reflux); (b) $Pd(PPh_3)_4$, DMF (90 °C); (c) (i) *n*-butyllithium, THF (−78 °C), (ii) $Sn(C_4H_9)_3Cl$; (d) $NaOH_{(aq)}$, $C_8H_{17}Br$, tributylammonium bromide, toluene, reflux; (e) *N*-bromosuccinimide, CH_3CO_2H, $CHCl_3$; (f) (i) BBr_3, DCM (0 °C), (ii) H_2O (ice); (g) K_2CO_3, DMF (90 °C).

scout target. Samples were dissolved in DCM with HABA (2-(4-hydroxyphenylazo)benzoic acid) matrix (1:10 DCM:HABA). IR spectra were recorded using a Perkin−Elmer Paragon 1000 Fourier transform−infrared (FT−IR) spectrometer. ^{1}H NMR spectra were recorded using a JEOL Lambda 400 spectrometer and an internal standard of tetramethylsilane (TMS. Aluminum-backed TLC plates coated with silica gel (60 F_{254}, Merck) were used to measure the progress of reactions. GC was carried out using a Chromopack CP3800 gas chromatogaph equipped with a 10 m CP-SIL 5CB column. Purification of intermediates and final products was mainly accomplished by gravity column chromatography,[1] using silica gel (40−63 μm, 60 Å) obtained from Fluorochem. The melting point and liquid-crystal transition temperatures of the solids prepared were measured using a Linkam 350 hot stage and control unit in conjunction with a Nikon E400 polarizing microscope. The transition temperatures of all the final products were confirmed using a Perkin−Elmer DSC-7 in conjunction with a TAC 7/3 instrument controller, using the peak measurement for the reported value of the transition temperatures. The extrapolated half C_p method was used to measure the value of T_g. Thin-layer chromatography (TLC), GC, and elemental analysis using a Fisons EA 1108 CHN were employed to measure the purity of intermediates and final compounds. The experimental details are found in the Supporting Information.

Experimental Methods. The mesomorphic behavior of compounds **1**−**9** was investigated between crossed polarizers using optical microscopy. The only phase observed was the nematic phase. Nematic droplets were observed on cooling from the isotropic liquid to form the Schlieren texture with two- and four-point brushes characteristic of the nematic phase along with optically extinct homeotropic areas. As the sample is cooled further, the texture often formed more optically extinct homeotropic areas, which indicates that the phase is optically uniaxial. The bi-refringent and homeotropic areas flashed brightly on mechanical disturbance. This behavior and the simultaneous presence of both the homeotropic and the Schlieren texture confirms that the mesophase observed is indeed a nematic phase, which is also consistent with the X-ray studies reported below.

The values for the liquid-crystal transition temperatures were confirmed by DSC. Good agreement (≈1−2 °C difference) with those values determined by optical microscopy was obtained. These values were determined twice on heating and cooling cycles on the same sample. Cooling/heating rates were 10 °C per minute. The values obtained on separate samples of the same compounds were reproducible, and negligible thermal degradation was observed even at relatively high temperatures (≈250 °C). The baseline of the spectra is relatively flat, and sharp transition peaks are observed. The melting point (Cr−N and Cr−I) and clearing point (N−I) are

both first order, as expected. A degree of supercooling below the melting point is often observed on the cooling cycle, and many of compounds **1**−**9** remain nematic at room temperature for several hours, although their melting points are often much higher than room temperature. This may be attributed, at least in part, to the high viscosity of the nematic phase of these materials and the presence of a glass transition for all of compounds **1**−**9**.

The photocurrent time-of-flight method was used to obtain the hole mobility. A glass/ITO/film/ITO/glass cell structure was used for most samples. The capillary flow of compounds **1**−**9** at isotropic temperature was found to be very slow (at least 30 min to fully fill the cells) as a result of the high viscosity. Hence, the cells were filled by vacuum-assisted movement of the compounds in their isotropic phase and then sealed. The thickness, l, of the thin films was about 3 μm. All samples were heated to isotropic before testing, and measurements were taken on cooling. An optical pulse from a N_2 laser (Laser Science VSL-337ND, 337 nm) incident on the thin film creates a thin sheet of electron−hole pairs next to the contact. The reactive mesogens did not undergo in situ photopolymerization during irradiation of N_2 laser optical pulses, as supported by the fact that their clearing points were unchanged after the experiments. A uniform electric field, $E = 3.3 \times 10^4$ V cm^{-1}, was applied across the organic layer, and the transit time, τ, was obtained from the intercept of the photocurrent plateau and tail plotted on a logarithmic scale. The carrier mobility, μ, was obtained from the equation $\mu = l/(E\tau)$. Compound **8** was uniaxially aligned using two rubbed polyimide surfaces to investigate the effect of macroscopic alignment on the mobility. LIQUICOAT PI from MERCK was used as an alignment layer. We used 3 wt % resin dissolved in the provided thinner. The mixture was spin-coated at 3000 rpm and hard baked at 300 °C for an hour to give an alignment layer of approximately 30 nm thickness, which was thin enough for tunneling of photoinduced charges to the electrode.

X-ray diffraction experiments were performed on a MAR345 diffractometer with a 2D image plate detector (Cu Kα radiation, graphite monochromator, $\lambda = 1.54$ Å). The samples were aligned in a magnetic field. Spacings were calculated by applying Bragg's Law: $2d\sin\theta = n\lambda$, where d is the spacing, θ is half the diffraction angle, and n is an integer. Integrated diffractograms are shown as a function of the scattering vector: $q \equiv 2\pi n/d = 4\pi\sin\theta/\lambda$.

III. Results and Discussion

Liquid Crystalline Behavior. Liquid crystals **1**−**9** shown in Tables 1 and 2 exhibit a nematic phase, and no other types of phases, such as smectic phases, were observed. Compounds **1**,[20] **3**,[20] **5**, **6**, **8**,[20] and **9** exhibit an enantiotropic nematic phase (above the melting point), and compounds **2**, **4**, and **7** possess a monotropic nematic phase (below the melting point). All the compounds exhibit a supercooled nematic state below the melting point but above a glass transition. The viscosity of the glassy state and also the nematic phase above the glassy state is very high because of the large aromatic core and the presence of four alkyl chains attached to the core in terminal and lateral positions. The high viscosity contributes to the considerable and unusual tendency of these relatively low-molar-mass compounds to vitrify, i.e., form a glassy nematic state. The different lengths of the terminal alkoxy chains and the different degree and position of chain branching prevents valid comparisons of the transition temperatures from being made. This is not the purpose of this study, and has been dealt with elsewhere for a much wider range of related materials.[19,20] However, it is clear that the melting points and clearing points are lowest for those compounds with a high degree of chain branching and long terminal chains. The thermal data also seem to suggest that the presence of a *cis*-carbon−carbon double bond has a smaller effect on the transition temperatures than a branching methyl group.

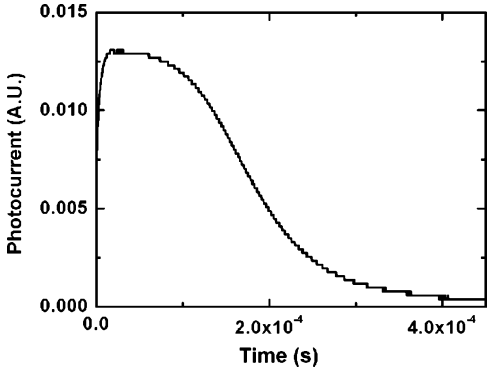

Figure 1. The photocurrent transients obtained from a 3 μm cell containing **5** at 50 °C on application of a voltage of 10 V.

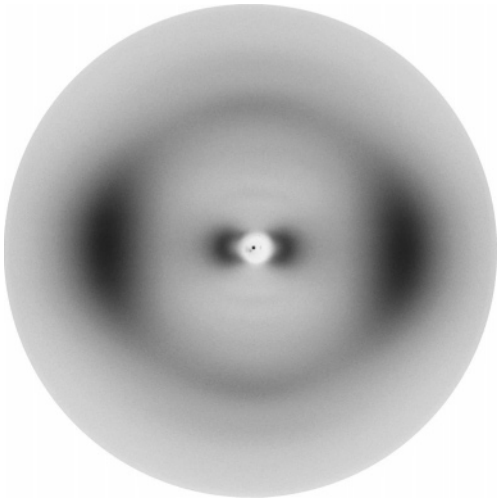

Figure 2. X-ray diffraction image of **9** at room temperature and aligned in a magnetic field. The magnetic field lies in the vertical direction.

Electronic Properties. Figure 1 shows a typical photocurrent transient from compound **5** on application of a voltage of 10 V. The transient has a well-defined plateau with low dispersion. Despite extremely large variations in the magnitude of the hole mobility, the total charge collected is approximately the same for all samples. This shows that the transients are not affected by deep trapping.

An X-ray diffraction pattern of compound **9** is shown in Figure 2. A magnetic field is used to align the material so that equatorial and meridional scattering correspond to the structure perpendicular and parallel to the director, respectively. Usually, calamitic nematic liquid crystals show a small-angle peak along the meridian corresponding to the average length of the rods.[21] This is not seen in Figure 2. Two pairs of equatorial diffuse scattering peaks are observed. This is also atypical of a nematic liquid crystal and cannot be explained by cybotactic smectic-like clusters within the nematic phase, because there is no scattering along the

(21) Ungar, G. *Physical Properties of Liquid Crystals: Nematics*; Dunmur, D. A., Fukuda, A., Luckhurst, G., Eds.; Institution of Electrical Engineers: Stevenage, U.K., 2000.

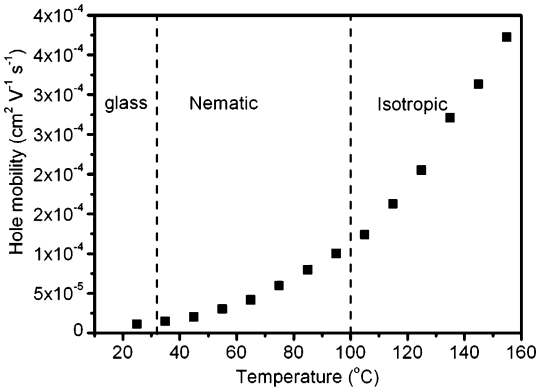

Figure 3. Hole mobility of **2** as a function of temperature.

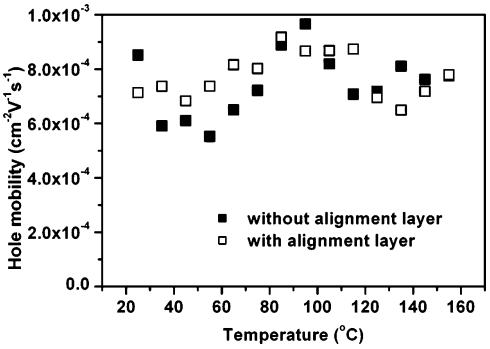

Figure 4. Comparison of mobilities between aligned and nonaligned samples of compound **8**.

meridian.[22] We believe this indicates local lamellar self-organization. The broad wide-angle diffraction peak gives a "short" intermolecular separation of 4.67 Å, a typical value for nematics. The small-angle diffraction peak in the equatorial plane corresponds to a *d* spacing of 22.5 Å. Molecular modeling gives a length of 12.2 Å for the octyl side chain at the 9-position of the central fluorene unit of the aromatic core. Hence, the "long" intermolecular spacing closely matches the combined length of two octyl groups. Both scattering peaks are diffuse and so are distinctly different to data from the recently observed lamellar nematic phase (Lam_N) in which the layered structures extend over a much larger spatial scale.[23,24] A similar local biaxial orientation has been proposed for explaining the X-ray diffraction results of polyfluorene in the nematic phase.[25] Local lamellar structures are observed even when compound **9** is not aligned by magnetic fields. The hopping probability of charge carriers depends on the intermolecular separation and so must be affected by lamellar organization. For now, we assume that charge carriers hop only between closely spaced molecules. Further study is required to characterize the effects of lamellar organization on carrier mobility.

Figure 3 shows a temperature-dependent increase in hole mobility for compound **2** from a room-temperature value of 1.1×10^{-5} cm^2 V^{-1} s^{-1}. The temperature dependence is typical of many non-liquid-crystalline materials with similarly low room-temperature mobility that show energetic disorder with thermal activation of the energetic barrier between neighboring chromophores.[26,27] The lack of discontinuity in the hole mobility between the nematic and isotropic phases suggests that hole mobility is insensitive to macroscopic orientational order. Similarly, compounds **1**−**7** show no discontinuities in charge mobility at the phase transitions, although different compounds have different temperature dependences. This is an unexpected result and substantially different from that found previously in smectics.[5,6] Electronic transport involves a series of intermolecular hops of carriers between the aromatic cores of nearest neighbors organized in small nematic domains, so that the local rather than the overall macroscopic order is more relevant.

The hopping probability depends on the overlap of the wave functions of the aromatic molecular cores and so has an inverse exponential dependence on the core separation. Hence, it is highly sensitive to the relative position and orientation of rodlike molecules. The local positional order present in the smectic layers is lost discontinuously at the transition from a smectic phase into the isotropic liquid, so a discontinuous change in mobility is expected and indeed observed. The insensitivity of mobility values to macroscopic order in the nematic phase of the kind of compound discussed here implies that molecular motion is still correlated on a local scale in the isotropic phase, so that the orientation of nearest neighbors remains roughly parallel in very small (submicrometer) domains, despite a macroscopic orientational order parameter of zero in the isotropic liquid. Indeed, such local dynamic order in the isotropic phase of nematic LCs is well-known,[29] and the correlation length decreases with temperature above the clearing point. It has also been suggested that nondispersive carrier transport of smectic LCs in the isotropic phase originates from short-range molecular order at that phase.[30] Figure 4 shows the temperature dependence of the hole mobility of a homogeneous uniaxially aligned and unaligned film of compound **8**. The field-effect mobility of nematic main chain polymers and oligomers is substantially higher for charge transport parallel rather than perpendicular to the nematic director.[28,16] Given that the time-of-flight method measures mobility normal to the substrate and there is no significant difference in values for the aligned and nonaligned case, we suggest that the directors of the unaligned have a planar orientation, albeit with random azimuthal alignment. Hence, in both cases, hole transport is perpendicular to the directors and a higher in-plane mobility would be expected for the uniaxially aligned sample.

Because the hole mobility is independent of macroscopic order, we can compare the transport properties of different compounds with the same aromatic core but different side groups and end groups, even though they have different liquid-crystal transition temperatures. We now show that the

(22) Bustamante, E. A. S.; Haase, W. *Liq. Cryst.* **1997**, *2*, 603.
(23) Patel, N. M.; Dodge, M. R.; Zhu, M. H.; Petschek, R. G.; Rosenblatt, C.; Prehm, M.; Tschierske, C. *Phys. Rev. Lett.* **2004**, *92*, 015501.
(24) Cheng, X.; Prehm, M.; Das, M.; Kain, J.; Baumeister, U.; Diele, S.; Leine, D.; Blume, A.; Tschierske, *C. J. Am. Chem. Soc.* **2003**, *125*, 10977.
(25) Grell, M.; Bradley, D. D. C.; Ungar, G.; Hill, J.; Whitehead, K. S. *Macromolecules* **1999**, *32*, 5810.
(26) Hannewald, K.; Bobbert, P. A. *Phys. Rev. B* **2004**, *69*, 075212.
(27) Bässler, H. *Phys. Status Solidi B* **1993**, *175*, 15.
(28) Sirringhaus, H.; Wilson, R. J.; Friend, R. H.; Inbasekaran, M.; Wu, W.; Woo, E. P.; Grell, M.; Bradley, D. D. C. *Appl. Phys. Lett*. **2000**, *77*, 406.
(29) De Gennes, P. E. *Phys. Lett.* **1969**, *A30*, 454.
(30) Shiyanovskaya, I.; Singer, K. D. *Phys. Rev. E* **2002**, *65*, 041715.

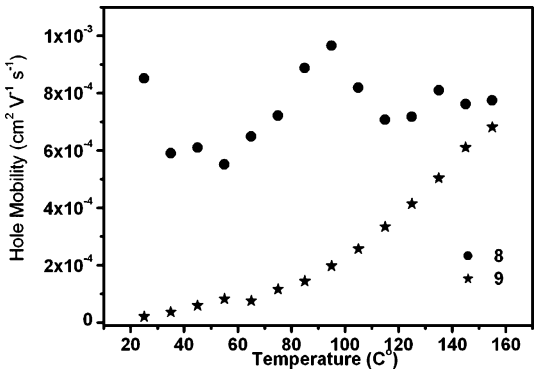

Figure 5. Hole mobility of **8** and **9** as a function of temperature.

nature of the lateral and terminal substituents of the nematic liquid crystals has a substantial effect on carrier mobility. The reactive mesogen **9** has been developed for electroluminescence,[14] and the photopolymerization of its 1,4-pentadiene side group gives rise to an insoluble polymer network film.[20] As shown in Figure 5, we found at least an order of magnitude difference in the hole mobility at 25 °C between compounds **8** and **9**, despite both materials having the same aromatic core and the same alkyl (C_8H_{17}) groups at the bridging benzylic position of the 9,9-dialkylfluorene moiety. Therefore, some feature of the terminal group must be responsible for the significantly lower mobility value of compound **9** compared to that of compound **8**.

The charge transport in energetically disordered organic materials is often interpreted using a Gaussian disorder model.[27] Compound **8** does not possess the polarizable branched diene end group and ester function (COO) present in the side chain of **9**, see Table 2. The presence of dipole moments in charge-transporting materials could increase the degree of energetic disorder via random polaron−dipole interactions and thus stabilize the polaron and decrease the charge-carrier mobility.[31,32] An experiment was carried out to check whether the polarizable nature of the ester or diene side group significantly reduces the hole mobility. As Table 1 shows, compounds **1**−**3** have the same aromatic core and branched end groups of similar length and shape, but have large differences in the polarizability of the end group. All three compounds have very similar hole mobility values at room temperature, i.e., 1.1×10^{-5}, 1.2×10^{-5}, and 1.7×10^{-5} cm^2 V^{-1} s^{-1}, respectively, as well as at elevated temperatures, as shown in Figure 6.

The room-temperature values are almost 2 orders of magnitude smaller than that of compound **4**, shown in Figure 7, which has nonbranched end chains. This further suggests that it is the shape of the end group rather than its polarizable nature that influences the hole transport.

As shown in Figure 8, the diene end group has a large volume of rotation. The end chains of nematic LCs interpenetrate the aromatic cores, so we expect that the bulkiness of the diene end group should increase the intermolecular separation and hence significantly lower the charge-carrier mobility. Figure 9 shows the radially integrated X-ray

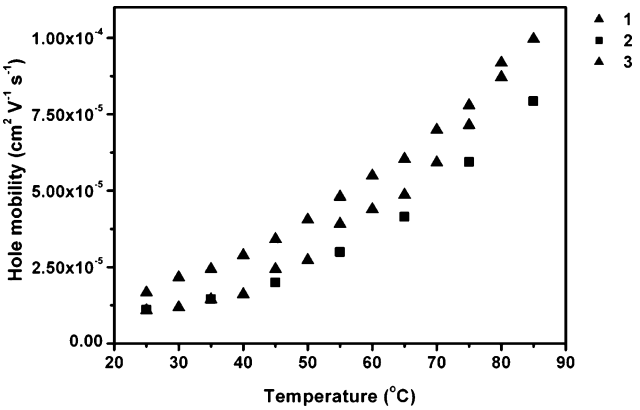

Figure 6. Hole mobility of **1**−**3** as a function of temperature.

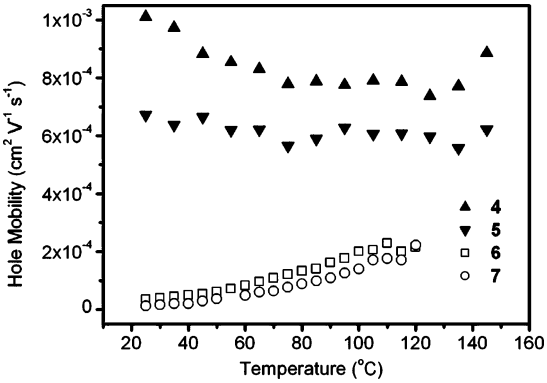

Figure 7. Hole mobility of **4**−**7** as a function of temperature.

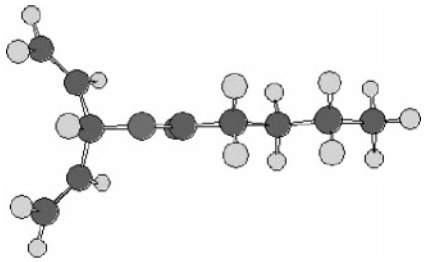

Figure 8. Molecular conformation of the aliphatic terminal chain containing a diene end group modeled using MOPAC AM1.

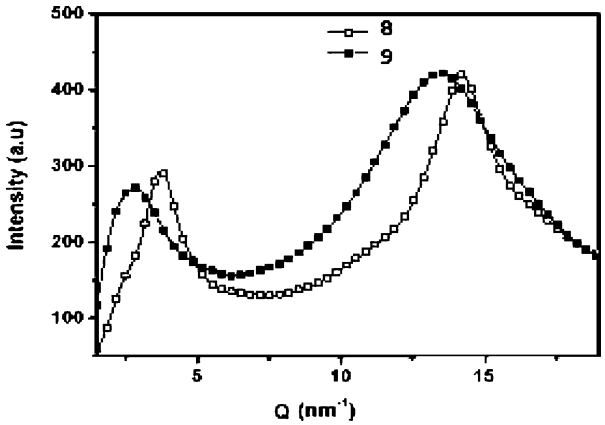

Figure 9. Radially integrated X-ray diffraction patterns of **8** and **9** as a function of q at room temperature.

diffraction pattern for compounds **8** and **9** at room temperature in the nematic glass and supercooled nematic phase, respectively. The wide-angle q value corresponds to intermolecular spacings of 4.43 and 4.67 Å for compounds **8** and **9**, respectively. Hence, we find that small differences in

(31) Young, R. H.; Sinicropi, J. A.; Fitzgerald, J. J. *J. Phys. Chem.* **1995**, *99*, 9497.
(32) Novikov, S. V.; Vannikov, A. V. *J. Imaging Sci. Technol.* **1994**, *38*, 355.

intermolecular spacing have an enormous effect on the charge-carrier mobility.

To further support this suggestion, we compare the transport properties of compounds **4**−**7**. Figure 7 shows that compound **5**, which contains branched side chains, has a much lower mobility at all temperatures compared to that of compound **4**, which has a nonbranched alkenyloxy chain containing a *cis*-carbon−carbon double bond. Compound **4** has a room-temperature hole mobility of 1.1×10^{-3} cm^2 V^{-1} s^{-1}, which represents the highest reported value for a low-molar-mass nematic LC to date. The *cis*-carbon−carbon double bond serves to maintain a linear conformation of the chain. This provides further confirmation of the correlation between different steric effects exerted by the terminal chains on the magnitude of the charge-carrier mobility.

Alkyl chains are present at the 9-position of the fluorene unit of compounds **1**−**9**, inducing a low melting point and ensuring good solubility of this class of electroluminescence materials in common organic solvents for the purposes of spin coating and subsequent room-temperature processing.[20] The values of the mobility at room temperature of compounds **6** and **7**, which contain octyl groups (C_8H_{17}) at the 9-position of the central fluorene core, are 5.4×10^{-5} and 2.9×10^{-5} cm^2 V^{-1} s^{-1}, respectively. As Figure 7 shows, these values are at least 1 order of magnitude less than those of the analogous compounds **4** and **5** containing much-shorter propyl groups (C_3H_7) at the fluorene 9-position, but which have similar end chains. Compounds with identical end chains could not be compared because of room-temperature crystallinity. X-ray diffraction of compounds **5** and **7** gives intermolecular distances of 3.91 and 4.36 Å so that the differences in carrier mobility can again be attributed to differences in the intermolecular distance. The temperature dependence of mobility shows two general trends: compounds with low room-temperature mobility are thermally activated, indicating energetic disorder.[27,28] Compounds **4**, **5**, and **9** have room-temperature mobility $> 5 \times 10^{-4}$ cm^{-2} V^{-1} s^{-1} and show smaller but more-random variation with temperature. Further investigations are required to explain the latter behavior.

We now consider the effect of the length of the aromatic core on charge transport. Compounds **6** and **8** contain six and eight aromatic rings, respectively, and both have identical side chains. The ionization potential of both materials is the same.[20] The room-temperature mobility of compound **8** is 7.5×10^{-4} cm^{-2} V^{-1} s^{-1}, a factor of 20 greater than that of compound **6**. This can be attributed to the increase in π-orbital overlap between adjacent molecules via the stronger van der Waals interactions. Indeed, a high hole mobility of 1.2×10^{-2} cm^{-2} V^{-1} s^{-1} is obtained for a nematic oligofluorene liquid crystal with 24 conjugated rings, in keeping with these results.[16] The same effect is observed in discotic LCs, for which mobility increases with increasing core size.[33] However, recent published work has suggested that such a mobility increase cannot be substantiated by an ever-increasing core size.[1] Hence, we believe that for such elongated nematic LCs, there also exists a saturation point whereby a further increase in the aromatic core length will not increase the charge mobility.

IV. Conclusions

The hole mobility of highly conjugated nematic LCs with a high degree of shape anisotropy does not primarily depend on the macroscopic ordering of the nematic phase, unlike in smectic or discotic LCs. Despite this, such nematic LCs are promising organic semiconductors; the extended conjugated backbone allows short intermolecular distances and a high degree of electronic wave function overlap, even in the isotropic state. Although even smaller separations are found for more-ordered LC phases,[4,34,35] these materials are less suitable for OLEDs because of quenching of luminescence by intermolecular interactions. The highest value for time-of-flight hole mobility (up to 1.0×10^{-3} cm^2 V^{-1} s^{-1}) in a small nematic LC is now reported, and small changes in intermolecular separation introduced by bulkier aliphatic groups can drastically alter this. Furthermore, such nematic LCs tend to lie in the substrate plane, so that even higher mobilities would be expected in field-effect-transistor configurations. It is clear from these studies that the position, size, and shape of terminal and lateral chains attached to the aromatic core have to be designed to induce a low melting point and high solubility of the materials in organic solvents, while inhibiting quenching by excimer formation (long chains) and at the same time facilitating a high charge-carrier mobility (short chains). An optimum balance is required for practical applications of such LC semiconductors. We also find a degree of local lamellar order. These findings should facilitate the design and synthesis of improved liquid crystals with much higher charge mobility for a range of applications, especially those using nematic polymer networks, such as OLEDs.

Acknowledgment. We thank G. Sowersby for technical support.

Supporting Information Available: Detail on the synthesis of **8** and **9**. This material is available free of charge via the Internet at http://pubs.acs.org".

CM0601335

(33) Craats, A. M.; Warman, J. M. *Adv. Mater.* **2001**, *13*, 130.
(34) Liu, C. Y.; Baird, A. J. *Nature* **2002**, *418*, 162.
(35) Gearba, R. L.; Lehmann, M.; Levin, J.; Ivanov, D. A.; Koch, M. H. J.; Barbera, J.; Debije, M. G.; Piris, J.; Geerts, Y. H. *Adv. Mater.* **2003**, *15*, 1614.